Chiang Mai J. Sci. 2020; 47(5) : 1068-1080
http://epg.science.cmu.ac.th/ejournal/
Contributed Paper

# Iron(II) Complexes Containing 1,2,4-Triazole-Pyridine and the Substituted Derivatives; Electronic Properties and Magnetic Moments

**Kristian Handoyo Sugiyarto*[a], Cornelia Budimarwanti [a] and Harold Andrew Goodwin [b]**

[a] Department of Chemistry Education, Yogyakarta State University (Universitas Negeri Yogyakarta), Jl. Colombo No.1., Yogyakarta 55281, Indonesia.

[b] The School of Chemistry, UNSW, Australia.

*Author for correspondence; e-mail: sugiyarto@uny.ac.id

Received: 24 November 2019
Revised: 21 January 2020
Accepted: 5 February 2020

## ABSTRACT

Iron(II) complexes of $[FeL_3][X]_2$, where L = *trzp*, 1-*mtrzp*, and 1,5-*dmtrzp*, X = $NO_3$ and I, and nickel(II) analogous, have been prepared and characterized in the electronic properties and magnetism. The complexes were found to be yellow to brownish for the dihydrates, $[FeL_3](X)_2{\cdot}2H_2O$. An additional complex of $[Fe(1,5\text{-}dmtrzp)_2Cl_2]$ was also isolated and found as an orange powder. The complexes, $[Fe(trzp)_3](NO_3)_2$, $[Fe(1,5\text{-}dmtrzp)_3](NO_3)_2$ and $[Fe(1,5\text{-}dmtrzp)_3](I)_2$ are fully paramagnetic at room temperature, the $\mu_{300K}$ being about 5.2 BM. These are, however, significantly temperature-dependent associated with thermally spin-state transition in iron(II), *singlet* $^1A_{1g}$ $(\ell.s)$ $\rightleftharpoons$ *quintet* $^5T_{2g}$ $(h.s)$, and the transitions are continuous and incomplete within the range of experimental temperature, down to 90K. The degree of incompleteness varies among them, and the least thermally induced was observed for $[Fe(1\text{-}mtrzp)_3](NO_3)_2$. The bis chlorido-ligand complex of $[Fe(1,5\text{-}dmtrzp)_2Cl_2]$, shows a normal high-spin nature down to ~ 100 K ($\mu_{100K}$ ~ 5.4 BM). The particular nickel complexes analogous show a normal paramagnet with $\mu_{300K}$ ~ 2.9 - 3.0 BM. The electronic spectrum for these complex reveals an octahedral geometry with $\nu_2/\nu_1$ being 1.58-1.59. The ligand field strength of about 11700-11800 $cm^{-1}$ is in the range in which the spin-state transition in the corresponding iron(II) complexes can be thermally induced.

**Keywords**: iron(II), nickel(II), spin-state, transition, triazole-pyridine

## 1. INTRODUCTION

The work on $[Fe^{II}N6]$ complexes, where Fe(II) central atom is surrounded with the six N donor atoms and associated with the well known dynamic spin state equilibrium of *singlet* $^1A_{1g}$ $(\ell.s)$ $\rightleftharpoons$ *quintet* $^5T_{2g}$ $(h.s)$ due to thermally induced are of interest to many researchers [e.g. 1-4]. Types of the transition in the solid-state have been observed to continue, discontinue, associated with hysteresis, complete, incomplete, and very rarely in two-steps. These are usually due to the general term of what is known as solid effects mainly with lattice forces in the crystal which may be influenced by the size, method of preparation, solvation, counter anion, and crystal defect [5,6].

So far, the continuous type of spin-state transition is usually much more observed than the discontinuous one. The discontinuous type and particularly associated with hysteresis is very rarely observed; this is being a prospective application in data storage and switching electronic devices [7-9].

The iron(II) complexes of pyridine-triazole and its derivatives (Figure 1), 2-(1,2,4-triazol-3-yl) pyridine, *trzp*, and 2-(1-methyl-1,2,4-triazol-3-yl) pyridine, 1-*mtrzp*, have been published to exhibit spin-state transition in iron(II) [10]. However, it was very brief and no further detailed study was then reported. Together with these two, another derivative, 2-(1,5-dimethyl-1,2,4-triazol-3-yl)pyridine, 1,5-*dmtrzp*, have been isolated as $[Fe(trzp)_3](X)_2 \cdot nH_2O$ and $[Fe(1\text{-}mtrzp)_3](X)_2 \cdot nH_2O$, where X = monovalent anion, Cl, $ClO_4$, $BF_4$, and $PF_6$ [11]. They exhibit a *singlet* $^1A_{1g}$ ($\ell .s$) $\rightleftharpoons$ *quintet* $^5T_{2g}$ ($h.s$) transition in iron(II) with gradual continuous type. The structural study of the *bidentate* showed the coordination of octahedral geometry through Fe-$N^{(4)}$ ($N_{triazole}$) and Fe-$N_{pyridine}$ [11], and thus following the *diimine* system [12]. The spin state was significantly anionic dependence associated with an incomplete transition within the range of experimental temperatures, and no hysteresis was observed in these systems [11].

Further studies with other anions might produce different types of spin-state transition in this system. Thus, the complexes of $[Fe(L)_3](X)_2$ (L = *trzp*, 1-*mtrzp*, and 1,5-*dmtrzp*, and X = $NO_3$, I, and Cl) were prepared along with the corresponding complexes of nickel(II) nitrate to reveal the ligand field strength for comparison [13, 14].

## 2. EXPERIMENTAL

### 2.1 Preparation of the Ligand and the Complexes

*Synthesis of 2-(hydrazidino)pyridine* and *2-(methyl-hydrazidino)pyridine*. The precursors of 2-(hydrazidino) pyridine and 2-(methyl-hydrazidino)pyridine were synthesized based on the modification of the method described by Kubota *et al.* [15] as the followings. To a well-stirred mixture of 2-(cyano)pyridine (0.05 mol) and slightly excess of hydrazine hydrate or methyl hydrazine hydrate (15 mL) was added ethanol (15 mL). The mixture was warmed for about 5 minutes and then allowed to stand at room temperature while stirring for about 24 hours. The solvent, ethanol, was then removed in a rotary evaporator, and the residue was extracted into benzene. The solution was then treated with charcoal while heating, filtered, and then concentrated with a rotary evaporator whereupon the yellow solid resulted. This was then re-crystallized in benzene.

*Synthesis of the ligand*. The triazole-pyridine was synthesized according to modification of method as described by Hage *et al.* [16] as follows. To about 15 mL of an ice-cold mixture of the relevant acid (formic or acetic acid) and carboxylic acid anhydride (1:16) was drop wisely added 2-(hydrazidino)-pyridine or 2-(methyl-hydrazidino)pyridine (about 0,03 mol). The mixture

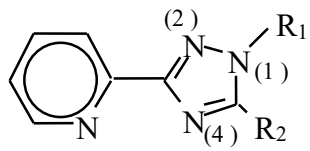


(1). *trzp*, $R_1 = R_2 = H$
(2). 1-*mtrzp*, $R_1 = CH_3$; $R_2 = H$
(3). 1,5-*dmtrzp*, $R_1 = R_2 = CH_3$

**Figure 1.** Pyridine-triazole derivatives (L).

was allowed to stand at room temperature for about 30 minutes and then refluxed for about 2-3 hours. The carboxylate was removed by rotary evaporator and the residue was neutralized with a solution of sodium carbonate (10%). The mixture was diluted with a minimum of water, extracted into chloroform, treated with charcoal and then concentrated by rotary evaporator whereupon white solid resulted (Figure 1). This was finally re-crystallized with chloroform-ether.

*Synthesis of the complexes*. To a solution of relevant ligand L (3 mmol) in a minimum of water was added an aqueous solution of $FeCl_2 \cdot 4H_2O$ or $NiCl_2 \cdot 6H_2O$ (1 mmol) under nitrogen atmosphere. The appropriate aqueous solution of either salt of either KI or $NaNO_3$ (slightly excess, 1.2 mmol) was then added whereupon the corresponding either iron(II) or Nickel(II) complex precipitated. The solid was filtered off, washed with a minimum of water and dried on aeration. For $[FeL_2Cl_2]$, it was directly precipitated on reducing the volume of the stoichiometric mixture of $FeCl_2 \cdot 4H_2O$ and 2L.

### 2.2 Physical Measurements

*Magnetism*. The magnetic data were obtained by a variable temperature Gouy balance of Newport which was calibrated with $CoHg(NCS)_4$. The diamagnetism of Pascal's constants were applied for correction in the calculation of all magnetic data [17]. The relationship of $\mu_{ef} = 2.828 \sqrt{(\chi'_M)T}$ BM, where $\chi'_M$= the corrected molar susceptibility and $T$ = temperature of the sample, was applied to the calculation of magnetic moment.

*Spectra*. Mössbauer spectra were recorded with a constant acceleration spectrometer in transmission mode equipped with $^{57}Co$ source in a palladium matrix, a Wissel drive unit, and a Norland multi-channel analyzer. The velocity scale was calibrated with sodium nitroprusside and metallic iron foil, and the isomer shift values quoted are relative to the midpoint of the iron spectrum at room temperature. The spectral parameters were then extracted from a least-squares fit of the data to the Lorentzian line shape.

Electronic spectra were recorded on a Zeiss PMQII spectrophotometer equipped with a particular accessory of diffuse reflectance. Powder samples were spread on filter paper supported with magnesium oxide for calibration of the spectra. Measurements at low-temperature were conducted with a special attachment of brass with silica glass windows. A stream of cold nitrogen gas was passed over the sealed fitting of the assembly to prevent condensation. The fitting was then set in contact with the base of an insulated brass Dewar which was filled with liquid nitrogen.

## 3. RESULTS AND DISCUSSION

### 3.1 Elemental Analysis of Ligands and Complexes

The ligands, *trzp*, 1-*mtrzp*, and 1,5-*dmtrzp* were prepared as white solids, and the C, H and N elemental analyses shown in Table 1 (listed together with their complexes) agree well with expected formulae. The purity of the ligands was confirmed by the $^1$H-*nmr* and $^{13}$C-*nmr* spectral data (Table 2). For the $^1$H-*nmr* spectra, the typical proton resonance for both N-methyl and C-methyl appear clearly at $\delta$ = 4 ppm and 2.5 ppm, respectively, while those for aromatic triazole and pyridine rings appear at $\delta$ = 7.00 - 9.00 ppm (Figure 2). The integral values of resonance are comparable with the corresponding formula of the ligand. For the $^{13}$C-*nmr* spectra, the typical carbon resonance for both N-methyl and C-methyl appear clearly at $\delta$ = 35 ppm and 12 ppm, respectively, while those for aromatic triazole and pyridine rings appear at 120-165 ppm. The stoichiometric reaction of either iron(II) or nickel(II) with ligand L, 1:3, and then followed by addition of an appropriate salts resulted in hydrated yellow to brownish-yellow complexes for $[FeL_3](X)_2$ and violet for $[NiL_3](X)_2$. While the orange chlorido complex was isolated by the stoichiometric mixture of iron(II) chloride with 1,5-*dmtrzp*, 1:2. The detailed color and elemental analyses of the complexes (Table 1) are considerably fit.

**Table 1.** Colour and elemental analysis of *ligand* and $[ML_3][X]_2.nH_2O$ (in % ); found figures are given below the calculated.

| Compounds | Colour | C | H | N | M |
|---|---|---|---|---|---|
| $C_7H_6N_4$, *trzp* (m.p., 151 $^0$C) | *white* | 57.53 | 4.14 | 38.34 | |
| | | 57.56 | 3.90 | 38.27 | |
| $C_8H_8N_4$, 1-*mtrzp* (m.p., 51-54 $^0$C) | *white* | 60.00 | 5.03 | 34.98 | |
| | | 59.92 | 5.30 | 34.87 | |
| $C_9H_{10}N_4$, 1,5-*dmtrzp* (m.p., 114 $^0$C) | *white* | 62.05 | 5.79 | 32.16 | |
| | | 61.52 | 5.63 | 31.66 | |
| $[Fe(trzp)_3](NO_3)_2{\cdot}2H_2O$ | *yellow* | 38.54 | 3.39 | 29.96 | 8.53 |
| | | 38.40 | 3.01 | 29.50 | 8.30 |
| $[Fe(trzp)_3](I)_2{\cdot}2.5H_2O$ | *brownish yellow* | 31.80 | 2.92 | 21.19 | 7.05 |
| | | 31.73 | 2.89 | 21.03 | 7.20 |
| $[Fe(1\text{-}mtrzp)_3](NO_3)_2{\cdot}2H_2O$ | *yellow-orange* | 41.39 | 4.05 | 28.15 | 8.02 |
| | | 41.50 | 3.90 | 27.94 | 8.2 |
| $[Fe(1,5\text{-}dmtrzp)_3](NO_3)_2{\cdot}2H_2O$ | *brownish yellow* | 43.91 | 4.64 | 26.55 | 7.56 |
| | | 44.11 | 4.56 | 26.35 | 7.77 |
| $[Fe(1,5\text{-}dmtrzp)_2Cl_2]$ | *orange* | 33.29 | 3.10 | 17.25 | 8.60 |
| | | 34.40 | 2.96 | 16.98 | 8.96 |
| $[Ni(trzp)_3](NO_3)_2$ | *violet* | 40.60 | 2.92 | 31.56 | 9.45 |
| | | 40.76 | 2.80 | 31.29 | 9.72 |
| $[Ni(1\text{-}mtrzp)_3](NO_3)_2{\cdot}2H_2O$ | *violet* | 41.22 | 4.03 | 28.04 | 8.39 |
| | | 41.56 | 3.95 | 27.91 | 8.64 |
| $[Ni(1,5\text{-}dmtrzp)_3](NO_3)_2{\cdot}2H_2O$ | *violet* | 43.73 | 4.62 | 26.44 | 7.91 |
| | | 44.00 | 4.23 | 26.12 | 8.06 |

**Table 2.** *Nmr* spectral data for ligands (in ppm, and integral values in bracket). The typical resonance for triazole ring, *s* = *singlet*, *bs* = *broad-singlet* (NH), and that for pyridine ring, *d* = *doublet*, *dd* = *doublet of doublet*, *dt* = *doublet of triplet*.

| $^1$H-*nmr* | | | *Resonance (in ppm)* | | | | | | |
|---|---|---|---|---|---|---|---|---|---|
| trzp | | | 7.4 (1) *dd* | 7.9 (1) *dt* | 8.1 (1) *s* | 8.3 (1) *d* | 8.8 (1) *dd* | 13.9 (1) *bs* | |
| 1-mtrzp | | 3.9 (3) *s* | 7.2 (1) *dd* | 7.7 (1) *dt* | 8.0 (1) *s* | 8.0 (1) *d* | 8.6 (1) *dd* | | |
| 1,5-dmtrzp | 2.5 (3) *s* | 3.9 (3) *s* | 7.2 (1) *dd* | 7.7 (1) *dt* | - | 8.0 (1) *d* | 8.7 (1) *dd* | | |
| $^{13}$C-*nmr* | | | *Resonance (in ppm)* | | | | | | |
| trzp | | | 122.0 | 125.0 | 137.8 | 146.6 | 149.5 | 151.8 | 154.9 |
| 1-mtrzp | | 36.3 | 121.3 | 123.7 | 136.7 | 144.4 | 149.5 | 149.8 | 162.1 |
| 1,5-dmtrzp | 11.9 | 35.4 | 121.1 | 123.6 | 136.6 | 144.8 | 149.9 | 153.2 | 160.1 |

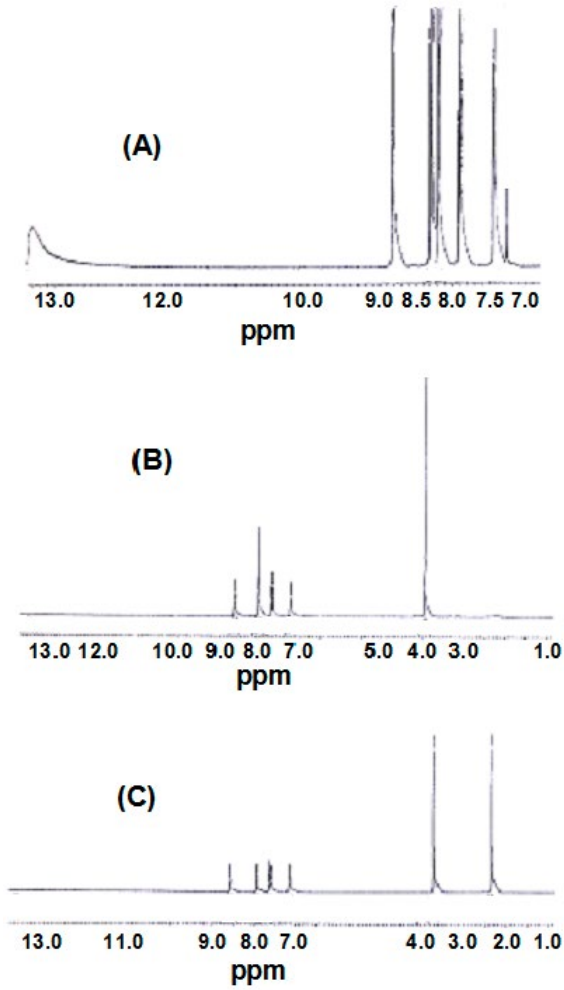


**Figure 2.** $^{1}$H-nmr Spectra for *trzp* (A), 1-*mtrzp* (B), and 1,5-*dmtrzp* (C).

### 3.2 Magnetic Property for the Iron(II)

All of the hydrated tris-triazole-pyridine iron(II) complexes were found to be normal high-spin with magnetic moment ~ 5.2 – 5.3 BM at room temperature. These are slightly higher than the theoretical moment of spin only ($\mu_S$ = 4.9 BM) as due to orbitally magnetic contribution, distortion of the cubic symmetry and spin-orbit coupling effect [18,19]. The detailed values are shown in Table 3.

The magnetic property for the un-substituted complex, [Fe(*trzp*)$_3$](X)$_2$, was significantly temperature-dependent, decreased gradually with decreasing temperatures, being down to 2.2 – 2.4 BM for the nitrate and 3.0 BM for the iodide at about 90 K (Figure 3). The change in moment due to change in temperature was reversible as shown in data collected in Table 3 which were listed according to the order of measurements. This is associated with the thermally spin state $^{1}A_{1g}$ ($\ell .s$) $\rightleftharpoons$ *quintet* $^{5}T_{2g}$ ($h.s$) transition in iron(II). Thus, the un-substituted ligand, *trzp*, can be considered to provide a "medium" ligand field about the metal atom. The transition continues and incomplete, leaving a significantly residual high spin fraction at low temperature (~ 90 K).

**Table 3.** Magnetic data for the iron(II) and nickel(II) complexes.

| $[Fe(trzp)_3](NO_3)_2.2H_2O$ | | | | | |
|---|---|---|---|---|---|
| Sample 1 | | | Sample 2 | | |
| **T/K** | **$\chi_M/10^{-6}$** | **μ/BM** | **T/K** | **$\chi_M/10^{-6}$** | **μ/BM** |
| 293.2 | 11634 | 5.22 | 293.2 | 11776 | 5.25 |
| 215.6 | 12542 | 4.52 | 215.6 | 12705 | 4.68 |
| 99 | 7286 | 2.40 | 99 | 5961 | 2.17 |
| 118.4 | 7251 | 2.62 | 118.4 | 6236 | 2.43 |
| 137.2 | 7617 | 2.81 | 137.2 | 6856 | 2.74 |
| 176.3 | 9800 | 3.72 | 156.5 | 8232 | 3.21 |
| 195.8 | 11285 | 4.20 | 176.3 | 9609 | 3.68 |
| 235.2 | 13013 | 4.95 | 195.8 | 11398 | 4.22 |
| 255 | 13066 | 5.16 | 235.2 | 12877 | 4.78 |
| 275 | 12437 | 5.23 | 255 | 12774 | 5.10 |
| 313.2 | 11180 | 5.29 | 275 | 12430 | 5.23 |
| | | | 313.2 | 11260 | 5.31 |
| $[Fe(trzp)_3](I)_2.2.5H_2O$ | | | | | |
| 303.2 | 11932 | 5.38 | 137.2 | 14352 | 3.97 |
| 235.2 | 14560 | 5.23 | 176.3 | 15315 | 4.65 |
| 195.8 | 15315 | 4.90 | 215.6 | 14925 | 5.07 |
| 156.5 | 15055 | 4.34 | 255 | 13650 | 5.28 |
| 118.1 | 13337 | 3.55 | 275 | 12791 | 5.30 |
| 89.1 | 12609 | 3.00 | 293.2 | 12349 | 5.38 |
| 99 | 12583 | 3.15 | 313.2 | 11594 | 5.39 |
| $[Ni(trzp)_3](NO_3)_2$ | | | | | |
| 303.2 | 3554 | 2.94 | 186.1 | 5767 | 2.93 |
| 99 | 10836 | 2.93 | 215.6 | 4981 | 2.93 |
| 127.6 | 8447 | 2.94 | 245 | 4369 | 2.93 |
| 156.5 | 6932 | 2.94 | 275 | 3903 | 2.93 |
| $[Fe(1\text{-}mtrzp)_3](NO_3)_2.2H_2O$ | | | | | |
| 303.2 | 11622 | 5.31 | 156.5 | 22323 | 5.28 |
| 186.1 | 18800 | 5.29 | 215.6 | 16338 | 5.30 |
| 89 | 34444 | 4.95 | 245 | 14274 | 5.30 |
| 127.6 | 27058 | 5.25 | | | |

| $[Ni(1\text{-}mtrzp)_3](NO_3)_2.2H_2O$ (θ = 16 K) | | | | | |
|---|---|---|---|---|---|
| **T/K** | **$\chi_M/10^{-6}$** | **μ/BM** | **T/K** | **$\chi_M/10^{-6}$** | **μ/BM** |
| 303.2 | 4100 | 3.15 | 186.1 | 6505 | 3.11 |
| 99 | 11526 | 3.01 | 215.6 | 5700 | 3.13 |
| 127.6 | 8792 | 3.00 | 245 | 5000 | 3.13 |
| 156.5 | 7241 | 3.01 | 275 | 4507 | 3.15 |
| $[Fe(1,5\text{-}dmtrzp)_3](NO_3)_2.2H_2O$ | | | | | |
| | Sample1 | | | Sample 2 | |
| 303.2 | 11138 | 5.20 | 293.2 | 11767 | 5.25 |
| 215.6 | 14252 | 4.96 | 215.6 | 13474 | 4.82 |
| 99 | 1364 | 1.04 | 156.5 | 4220 | 2.30 |
| 118.4 | 1932 | 1.35 | 99 | 2210 | 1.32 |
| 137.2 | 2745 | 1.73 | 118.4 | 2589 | 1.56 |
| 156.5 | 5967 | 2.73 | 137.2 | 3044 | 1.83 |
| 176.3 | 10353 | 3.83 | 176.3 | 6799 | 3.10 |
| 195.8 | 13087 | 4.53 | 195.8 | 10326 | 4.02 |
| 245 | 13521 | 5.02 | 245 | 13701 | 5.18 |
| 275 | 12248 | 5.19 | 275 | 12564 | 5.26 |
| 323.2 | 10500 | 5.21 | 303.2 | 11767 | 5.34 |
| $[Fe(1,5\text{-}dmtrzp)_2Cl_2]$ Sample 1 | | | | | |
| 303.2 | 12142 | 5.42 | 186.1 | 19710 | 5.42 |
| 89 | 41827 | 5.46 | 215.6 | 17159 | 5.43 |
| 118.1 | 31053 | 5.42 | 245 | 15072 | 5.43 |
| 156.5 | 23505 | 5.42 | 275 | 13343 | 5.42 |
| $[Fe(1,5\text{-}dmtrzp)_2Cl_2]$ Sample 2 | | | | | |
| 303.2 | 11556 | 5.29 | 99 | 36087 | 5.34 |
| | | | | | |
| $[Ni(1,5\text{-}dmtrzp)_3](NO_3)_2.2H_2O$ | | | | | |
| 303.2 | 3232 | 2.80 | 186.1 | 5407 | 2.84 |
| 99 | 10761 | 2.91 | 215.6 | 4571 | 2.81 |
| 127.6 | 8335 | 2.91 | 245 | 4110 | 2.84 |
| 156.5 | 6662 | 2.89 | 275 | 3567 | 2.80 |

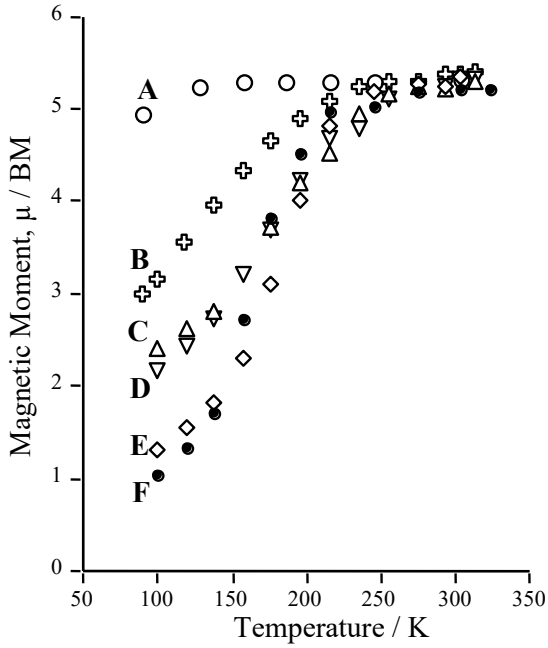


**Figure 3**. Magnetic moment *vs* Temperature for: (A) $[Fe(1\text{-}mtrzp)_3](NO_3)_2$, (B) $[Fe(trzp)_3](I)_2.2.5H_2O$, (C) $[Fe(trzp)_3](NO_3)_2{\cdot}2H_2O$ - Sample 1, (D) $[Fe(trzp)_3](NO_3)_2{\cdot}2H_2O$ - Sample 2, (E) $[Fe(1,5\text{-}dmtrzp)_3](NO_3)_2{\cdot}2H_2O$ - Sample 1, (F) $[Fe(1,5\text{-}dmtrzp)_3](NO_3)_2{\cdot}2H_2O$ - Sample 2.

The trend of the curve suggests that a fully low spin value for this complex will never be reached at lower temperatures.

The magnetic property for the dimethyl substituted complex, $[Fe(1,5\text{-}dmtrzp)_3](X)_2$, was also quite similar to that for the un-substituted, $[Fe(trzp)_3](X)_2$ as shown in Figure 3 and Table 3. The transition temperature, however, is relatively higher for the former, the residual high spin fraction being much lesser and thus the transition is nearly complete at low temperature (~ 99 K). This suggests that the insertion of two methyl groups, one to be at the carbon atom number 5 in triazole ring and thus adjacent to $N^{(4)}$-donor atom, does not lower the strength of nitrogen-metal coordination associated with the steric effect. Conversely, the insertion of the two methyl groups seems to increase the basicity of the triazole ring, and hence the strength of nitrogen-metal coordination which is, in turn, resulting in steric hindrance.

For the monomethyl substituted complex as for $[Fe(1\text{-}mtrzp)_3](X)_2$, however, there was simply no change in magnetic moment and thus found to be normal high-spin at least down to ~ 216 K. At lower temperatures, a very slight change in the moment occurred with a value of 4.95 BM at 89 K, and this trend suggests that lower magnetic moments would be observed at further lowering temperatures (Figure 3, Table 3). Thus, the complex is thermally more stabilized with the quintet state than the other two complexes, and partial transition to low-spin associated with the spin-state transition in iron(II) seems to observe at temperatures lower than 89 K.

Hence, the magnetic data suggest that the Fe-N coordination in 1-*mtrzp* is weaker than that in *trzp* and 1,5-*dmtrzp*. The entering methyl group at $N^{(1)}$ adjacent to $N^{(2)}$ atom in the triazole ring, therefore, can be considered to increase the steric effect, which is, in turn, weakening Fe-$N^{(4)}$

coordination at least in this instance. The next entering methyl group at $C^{(5)}$ adjacent to $N^{(4)}$ donor atom should, therefore, increase Lewis basicity of the triazole ring resulting in strengthening Fe-$N^{(4)}$ coordination. This compensates the steric effect due to $N^{(1)}$-methyl as well as $C^{(5)}$-methyl groups, giving rise to no difference in coordinating strength from the un-substituted *trzp*.

It has been shown, however, that the introduction of methyl substituents into a five-membered heterocycle ring including 1,2,4-triazole generally creates less steric interference to coordination than a similar introduction into a pyridine ring [20]. This is due at least in part to the actual geometry of the five-membered ring being directed further away from the donor atom than in a six-membered ring. Another further consequence of this substitution is that it can lead to increased *inter-ligand* repulsions which may affect the net-actual ligand field strength as well as influence the geometry coordination environment. In the present complexes, these effects seem to be approximately balanced so that all the three ligands provide comparable fields about iron(II) for a spin transition to occur. As a result, a meridional configuration is favoured as observed in the structure of $[Fe(1,5\text{-dmtrzp})_3](BF_4)_2$ with a wider angle in directing the methyl group further away from the metal atom and thereby reducing the steric barrier to coordination. Thus, the effects of the methyl substituents are obviously relatively minor in terms of influencing the field strength of the ligand. In the light of this it is not so surprising that the electronic properties of the derivatives of *trzp* and 1,5-*dmtrzp* are not significantly different [11].

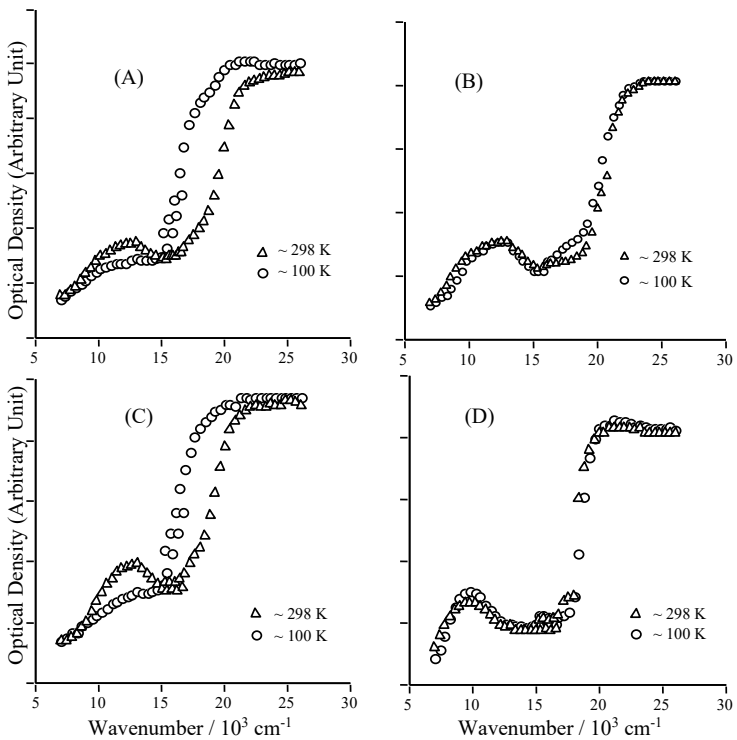


**Figure 4.** Diffuse reflectance spectra for : A.$[Fe(trzp)_3](NO_3)_2$, B.$[Fe(1\text{-}mtrzp)_3](NO_3)_2$, C.$[Fe(1,5\text{-}dmtrzp)_3](NO_3)_2$, D.$[Fe(1,5\text{-}dmtrzp)_2Cl_2]$.

Bis-(1,5-dimethyl-triazol-3yl)pyridinedichloridoiron(II), [Fe(1,5-*dmtrzp*)$_2$Cl$_2$] was found to be purely high spin down to ~ 90 K as expected. The magnetic moment which is about 5.4 BM at room temperature follows the common Currie-Weiss rule [21]. The replacement of a bidentate 1,5-*dmtrzp* by the very weak ligand field strength of dichlorido results in totally weak ligand field strength in the molecular complex, and therefore, purely paramagnet.

### 3.3 Electronic Spectra for the Iron(II)

The electronic spectra of [FeL$_3$](X)$_2$, (L = *trzp*, 1-*mtrzp*, and 1,5-*dmtrzp*), show a similar pattern (Figure 4), revealing two main bands. The low energy asymmetric band centered at about 12500 cm$^{-1}$ should correspond to the high-spin ligand field band, being in line with magnetic data ($\mu_{300K}$ = 5.3 BM). This band is usually assigned as an allowed spin transition, $^5T_{2g} \rightarrow {}^5E_g$. This assignment agrees well with that for [Fe(*ptz*)$_6$](BF$_4$)$_2$ (*ptz* = 1-*propyl tetrazole*) which was observed at about 12250 cm$^{-1}$ [22]. The asymmetric band is not surprising, and it is due to a well known Jahn-Teller effect associated with the "asymmetric" configuration of $^5T_{2g}$ ground state, $(t_{2g})^4 (e_g)^2$ [23]. The much higher energy band with quite strong intensity is centered at about 21000 - 23000 cm$^{-1}$, and this is frequently attributed as charge transfer metal to ligand, $t_{2(M)} \rightarrow \pi^*_{(L)}$ [23]. Due to the accumulation of negative charge from the six electron pairs of $N_{donor}$-ligand surrounding the central atom, the metal-ligand back bond then resulted [12].

The intensity and also the position of the absorption bands for these complexes, in fact, were found to be temperature-dependent, being significant for the un-substituted (*trzp*) and the dimethyl substituted (1,5-*dmtrzp*) complexes, but much less significant for the N-methyl substituted (1-*mtrzp*) as shown in Figure 4. Thus, at about 100 K, the intensity of the high-spin ligand field band was reduced significantly to nearly diminished, but that of the charge transfer band was increased and shifted to lower energy. These changes should be due to the decreasing high-spin but simultaneously increasing low-spin populations of iron(II) at low temperature, which is certainly in line with the magnetic data, $\mu_{99K}$ = 1.0 – 2.4 BM for [Fe(trz)$_3$]$^{2+}$ and [Fe(1,5-*dmtrzp*)$_3$]$^{2+}$, and 4.9 BM for [Fe(1-*mtrzp*)$_3$]$^{2+}$. The increase in intensity and the shift to the lower energy of the charge transfer band, on the other hand, was merely associated with an increase in the low-spin population of iron(II) in which the $t_{2(M)} \rightarrow \pi^*_{(L)}$ take place more facile due to reducing Fe-N bond length. Hence, the electronic spectral properties for these complexes support the assignment of spin-state transition in iron(II) indicated by magnetic data.

Moreover, another shoulder centered at about 18000 cm$^{-1}$ appears clearly with high intensity in the spectra for [Fe(*trzp*)$_3$]$^{2+}$ and [Fe(1,5-*dmtrzp*)$_3$]$^{2+}$ but with much lower intensity in that for [Fe(1-*mtrzp*)$_3$]$^{2+}$. These bands may not be associated with the low-spin ligand field band, though the similar value of the low-spin ligand field band was observed for [Fe(*ptz*)$_6$](BF$_4$)$_2$ [24], rather than another charge transfer band due to different coordination energy for Fe-$N_{triazole}$ from Fe-$N_{pyridine}$. The expected low-spin ligand field band lies about this region, but it can not be resolved since its intensity should be much lower than the charge transfer band.

Structural data for [Fe(1,5-*dmtrzp*)$_3$](BF$_4$)$_2$ reveals that the bond length for Fe-$N_{pyridine}$ was found to be longer than that for Fe-$N_{triazole}$ [11], and this seems to be a general observation for similar bidentate system, [Fe$^{II}$N$_6$], in which the distance for Fe-N($_{six\text{-}member\ ring}$) was always longer than that for Fe-N($_{five\text{-}member\ ring}$) [20]. Consequently, the charge transfer for Fe-$N_{triazole}$ would be more facile or lesser energy than that for Fe-$N_{pyridine}$ as observed in these complexes.

Qualitatively, a thermochromism from yellow to brownish on cooling down to 90 K was observed for both [Fe(*trzp*)$_3$]$^{2+}$ and [Fe(1,5-*dmtrzp*)$_3$]$^{2+}$, but from yellow-orange to only slightly deeper for [Fe(1-*mtrzp*)$_3$]$^{2+}$. This is, therefore, in line with

and responsible for the change in the electronic spectral pattern with temperature.

For [Fe(1,5-*dmtrzp*)$_2$Cl$_2$], the electronic spectrum (Figure 4D) reveals a high-spin ligand field band centered at about 10000 cm$^{-1}$, being significantly lower than those for the other two complexes. The second strong absorption centered at about 20500 cm$^{-1}$ which is assigned as the charge transfer band, $t_{2(M)} \rightarrow \pi^*_{(L)}$, should be responsible for the strong orange color. No change in intensity nor pattern with temperature was observed for this spectrum, and thus, consistent with the purely high spin nature for this instance.

### 3.4 Mössbauer Spectra for the Iron(II)

Confirmation for the *singlet* $^1A_{1g}$ ($\ell.s$) $\rightleftharpoons$ *quintet* $^5T_{2g}$ ($h.s$) equilibrium in iron(II) was significantly supported by the Mössbauer spectral property. This has been reported in this system for the tetrafluoroborate, perchlorate, and hexafluorophosphate [11]. Due to technical problem, the Mössbauer data could be recorded at room temperature only for [Fe(*trzp*)$_3$](NO$_3$)$_2$·2H$_2$O, and [Fe(1-*mtrzp*)$_3$](NO$_3$)$_2$ as shown in Figure 5. Both spectra reveal two doublets, the major (I) and the minor (II), the parameters being $\Delta E_Q$ = 1.39 mm s$^{-1}$ and $\delta_{is}$ = 0.84 mm s$^{-1}$ for doublet I (major), and $\Delta E_Q$ = 3.44 mm s$^{-1}$ and $\delta_{is}$ = 0.91 mm s$^{-1}$ for doublet II (minor) for [Fe(*trzp*)$_3$](NO$_3$)$_2$·2H$_2$O (Figure 4A), and $\Delta E_Q$ = 0.76 mm s$^{-1}$ and $\delta_{is}$ = 0.83 mm s$^{-1}$ for doublet I (major), and $\Delta E_Q$ = 1.85 mm s$^{-1}$ and $\delta_{is}$ = 0.85 mm s$^{-1}$ for doublet II (minor) for [Fe(1-*mtrzp*)$_3$](NO$_3$)$_2$ (Figure 4B). The typical spectra for both are principally the

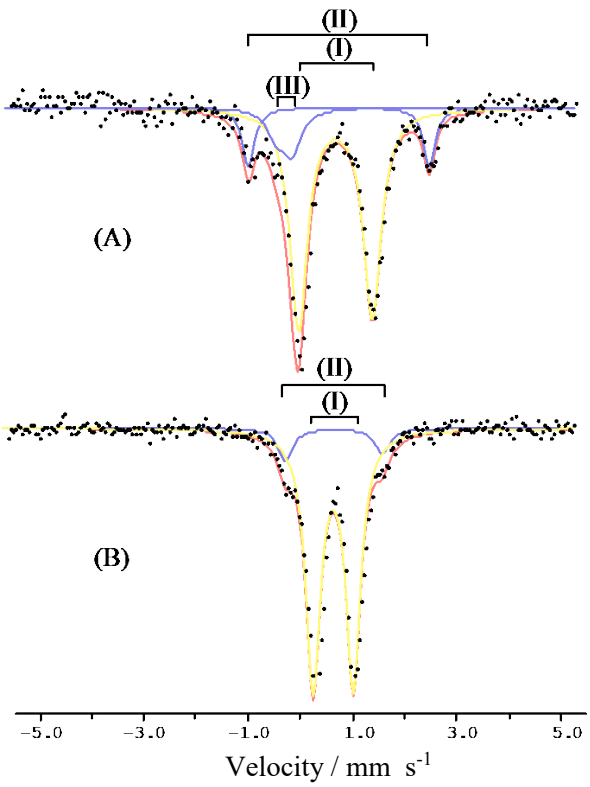


**Figure 5.** Mössbauer spectra at ~ 298K for: (A) [Fe(*trzp*)$_3$](NO$_3$)$_2$·2H$_2$O, (B) [Fe(1-*mtrzp*)$_3$](NO$_3$)$_2$.

same as those for other complexes with different counter anions [11].

All of the parameters are normal for the high-spin iron(II) [25]. The typical two doublet sites of high-spin iron(II), major(I) and minor(II), suggest that the two geometric isomers of facial and meridional may be present in these instances, and thus giving rise to significantly different in Mössbauer parameters particularly the quadrupole splitting. The facial isomer has a lower symmetry than the meridional one and therefore has the greater quadrupole splitting (doublet II-minor). Hence, the complexes may be dominated by the meridional isomer (doublet I, major).

The predominant two doublets in the spectra are consistent with the paramagnetic data in these instances. For $[Fe(trzp)_3](NO_3)_2{\cdot}2H_2O$, however, the spectrum shows an asymmetric resonance for one of the low-velocity major lines (III) which can not be accurately extracted, but certainly indicative of low spin iron(II). Thus at room temperature, this complex seems to contain a very small low spin population of iron(II) though its magnetic moment was found to be reasonably high, 5.2 BM. The low spin fraction at room temperature was not observed for the dehydrated hexafluorophosphate, perchlorate, and tetrafluoroborate [11]. For this reason, the presence of (di)hydrate in the complex might form such kind of hydrogen bonding *via* $H_2O\text{-}HN_{(1)\text{-}trz}$, thereby resulting in a slightly stronger $Fe\text{-}N_{trz}$ coordination, giving rise to a low spin state to present.

### 3.5 Magnetic and Electronic Properties for the Nickel(II)

The magnetic moment of the nickel(II) analogous complexes, $[Ni(L)_3](NO_3)_2{\cdot}2H_2O$ (L = *trzp*, 1-*mtrzp*, and 1,5-*dmtrzp*), were found to be 2.8-3.15 BM at 303 K ($\theta$ = 16 K ; Table 3). These values are normal for an octahedral nickel(II) complex which corresponds to two unpaired electrons in the ground state $(t_{2g})^6 (e_g)^2$ configuration; a slightly orbital contribution *via* spin-orbit coupling is common for nickel(II) and this was observed

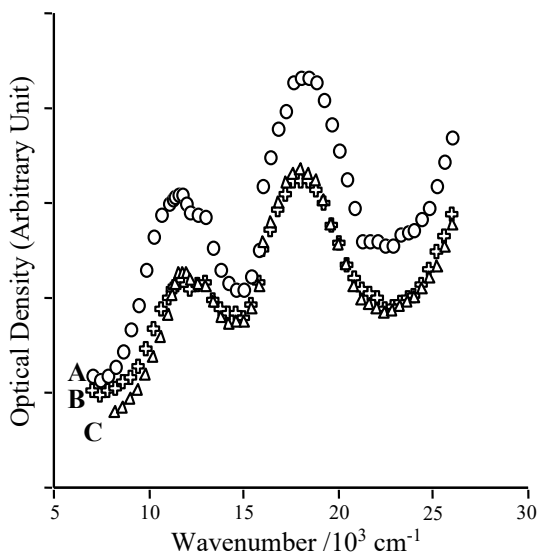


**Figure 6.** Diffuse reflectance spectra at ~ 298 K: A = $[Ni(trzp)_3](NO_3)_2$, B = $[Ni(1,5\text{-}dmtrzp)_3](NO_3)_2$, C = $[Ni(1\text{-}mtrzp)_3](NO_3)_2$.

for L = 1-*mtrzp*. The diffuse reflectance spectra for these complexes as shown in Figure 6 show a similar pattern revealing the two typical ligand field bands. The first ($\nu_1$) and the second ($\nu_2$) bands associated with the allowed spin transitions, $^3A_2 \rightarrow {}^3T_2$ and $^3A_2 \rightarrow {}^3T_1(F)$ are centered at about 11450 and 18100-18200 $cm^{-1}$, respectively. A typical shoulder about the first ligand field band was observed at ~ 12800 - 13000 $cm^{-1}$ and it is assigned as $^3A_2 \rightarrow {}^1E$ transition. The ratio ($\nu_2/\nu_1$) values of about 1.58-1.59 are lesser than that for a regular octahedral geometry (1.62) as suggested by Lever [26]. Thus, the complexes adopt primarily a distorted octahedral configuration. The ionic radii of nickel(II) lie between that of low-spin and high-spin iron(II), therefore, the corresponding iron(II) complexes are expected to adopt a similar geometry, and such distortion is indicated by their asymmetric high-spin ligand field bands.

The ligand field strength about the nickel(II) complex is indicated primarily by $\nu_1$, and thus it is relatively the same for these instances. The value of $\nu_1$ (11450$cm^{-1}$) is in the critical range proposed by Robinson *et al,* [13], namely 10400-12380 $cm^{-1}$, in which the corresponding iron(II) complexes undergo a spin-state transition as observed for these instances.

From the ligand field absorptions for these nickel(II) complexes, it can be deduced that insertion of the mono-methyl and di-methyl groups in the triazole ring do not reduce the corresponding ligand field strength, and thus it is clearly in line with the ground states observed for the corresponding iron(II) complexes.

## 4. Conclusions

The complexes of $[ML_3](X)_2$ (M = Fe , and Ni; L = *trzp*, 1-*mtrzp*, and 1,5-*dmtrzp*; X = $NO_3$ and I) and $[Fe(1,5\text{-}dmtrzp)_2Cl_2]$ were isolated and characterized in magnetic and electronic spectral properties. All of the iron(II) complexes are high spin at room temperature and exhibit spin transition associated with *singlet* $^1A_{1g}(\ell .s)$ $\rightleftharpoons$ *quintet* $^5T_{2g}$ (*h.s*) equilibrium except for the dichlorido complex which is merely fully high spin. The transition is gradual and incomplete down to ~ 99 K. The nickel(II) complexes are normal paramagnetic associated with two unpaired electrons and adopt a distorted octahedral configuration with a ratio of $\nu_2/\nu_1$ being 1.58-1.59.

## References


[1] Sugiyarto K.H. and Goodwin H.A., *Chiang Mai J. Sci.,* 2019; **46(4)**: 756-765.

[2] Kitazawa T., *Crystals,* 2019; **9(8)**: 382-385. DOI 10.3390/cryst9080382.

[3] Gütlich P., Gaspar A.B. and Garcia Y., *Beilstein J. Org. Chem.,* 2013; **9**: 342-391. DOI 10.3762/bjoc.9.39.

[4] Chastanet G., Lorenc M., Bertoni R. and Desplanches C., *C. R. Chim.,* 2018; **21(12)**: 1075-1094. DOI 10.1016/j.crci.2018.02.011.

[5] Gütlich P., *Mössbauer Spectroscopy and Its Chemical Applications (Advances in Chemistry Series),* 1st Edn., American Chemical Society, 1981. DOI 10.1021/ba-1981-0194.ch019.

[6] Sertphon D., Harding P., Murray K., Moubaraki B., Neville S., Liu, L. Telfer S.G. and Harding D., *Crystals,* 2019; **9(2)**, 116-127. DOI 10.3390/cryst9020116.

[7] Khan O., Kröber J. and Jay C., *Adv. Mater.*, 1992; **4**: 718-728. DOI org/10.1002/adma.19920041103.

[8] Kahn O. and Codjovi E., *Philos. Trans. R. Soc. London, Ser. A*, 1996; **354(1706)**: 359-379. DOI 10.1098/rsta.1996.0012.

[9] Senthil Kumar K. and Ruben M., *Coord. Chem. Rev.,* 2017; **346**: 176-205. DOI 10.1016/j.ccr.2017.03.024.

[10] Stupik P., Reiff W.M., Hage R., Jacobs J., Haasnoot J.G. and Reedijk J., *Hyperfine Interact.,* 1988; **40(1-4)**: 343-345. DOI 10.1007/bf02049113.

[11] Sugiyarto K.H., Craig D.C., Rae A.D. and

Goodwin H.A., *Aust. J. Chem.,* 1995; **48**: 35-54. DOI org/10.1071/CH9950035.

[12] Goodwin H.A., *Top. Curr. Chem*., 2004; **233**: 59-90; DOI 10.1007/b13529.

[13] Robinson M.A., Curry J.D. and Busch D.H., *Inorg. Chem.,* 1963; **2(6)**: 1178-1181. DOI 10.1021/ic50010a021.

[14] Phan H., Hrudka J.J., Igimbayeva D., Lawson Daku L.M. and Shatruk M., *J. Am. Chem. Soc.,* 2017; **139(18)**: 6437-6447. DOI 10.1021/jacs.7b02098.

[15] Kubota S., Uda M. and Nakagawa T., *J. Heterocyclic Chem.,* 1975; **12(5)**: 855-860. DOI 10.1002/jhet.5570120509.

[16] Hage R., Prins R., Haasnoot J.G., Reedijk J. and Vos J.G., *J. Chem. Soc., Dalton Trans.,* 1987; **6**: 1389-1395. DOI 10.1039/dt9870001389.

[17] Figgis B.N. and Lewis J., *Modern Coordination Chemistry*, in Lewis J. and Wilkins R.G., Eds., Interscience Publishers Inc., New York, 1960: 400-454.

[18] Alouani M., Baadji N., Abdelouahed S., Bengone O. and Dreyssé H., *Lect. Notes Phys.,* 2009; **795**: 309-341. DOI 10.1007/978-3-642-04650-6_9.

[19] Meyer J., Tombers M., van Wüllen C., Niedner-Schatteburg G., Peredkov S., Eberhardt W., Neeb M., Palutke S., Martins M. and Wurth W., *J. Chem. Phys.,* 2015; **143(10)**: 104302. DOI 10.1063/1.4929482.

[20] Baker A.T., Goodwin H.A. and Rae A.D., *Inorg. Chem.,* 1987; **26(21)**: 3513-3519. DOI 10.1021/ic00268a020.

[21] Gupta A. and Yan D., *Mineral Processing Design and Operations*, 2nd Edn., Elsevier B.V., 2016. DOI:10.1016/b978-0-444-63589-1.00017-4

[22] Hauser A., Vef A. and Adler P., *J. Chem. Phys.,* 1991; **95(12)**: 8710-8717. DOI 10.1063/1.461255.

[23] House J.E., *Inorganic Chemistry,* 2nd Edn., Academic Press, Illinois, 2013. DOI 10.1016/b978-0-12-385110-9.00017-0.

[24] Hauser A., Gütlich P. and Spiering H., *Inorg. Chem.*, 1986; **24**: 4245-4248. DOI 10.1021/ic00243a036.

[25] Goodwin H.A., *Coord. Chem. Rev.*, 1976; **18(3)**: 293-325. DOI 10.1016/s0010-8545(00)80430-0.

[26] Lever A.B.P., *Inorganic Electronic Spectroscopy*, Elsevier Publishing Company, Amsterdam. 1968.